Pressurized Water Bearing Solves Environmental Problems

Carlo F. Luri, Bently Biofuels Company

The position of the bearings in the machine train often puts oil in close proximity to the path of water through the hydro turbine. This novel bearing design uses externally pressurized water lubrication to eliminate the source of this potential environmental liability and improve the rotordynamic performance of many types of high and low speed machinery.

Low pressure oil lubricated hydrodynamic bearings were specified 100 years ago as original equipment on Southern California Edison's hydro turbines. While low pressure oil bearings have been adequate for this and many other installations, the advent of stricter environmental regulations and the cost of safety, health, and environmental compliance make the continued use of these bearings in any hydro turbine application a risky proposition.

Recent improvements have allowed water lubricated externally pressurized bearings to replace oil lubricated hydrodynamic (internally pressurized) bearings in many applications. For the water power industry, the primary advantage of the externally pressurized bearing is the option to use an environmentally benign fluid, such as water, for lubrication without loss of load carrying capacity, efficiency, or reliability. A properly engineered externally pressurized bearing also results in better stability and control of the vibration response to dynamic forces acting on the rotor.

Early History of Fluid Film Bearing Lubrication

A few years before the early hydro turbines were installed, the expansion of the railroads in the western United States drove the

by direct contact between the shaft and axle. This early theory, based on the work of Frenchman Charles Augustine Coulomb, predicted that once the surfaces were in motion, friction should be nearly independent of velocity.

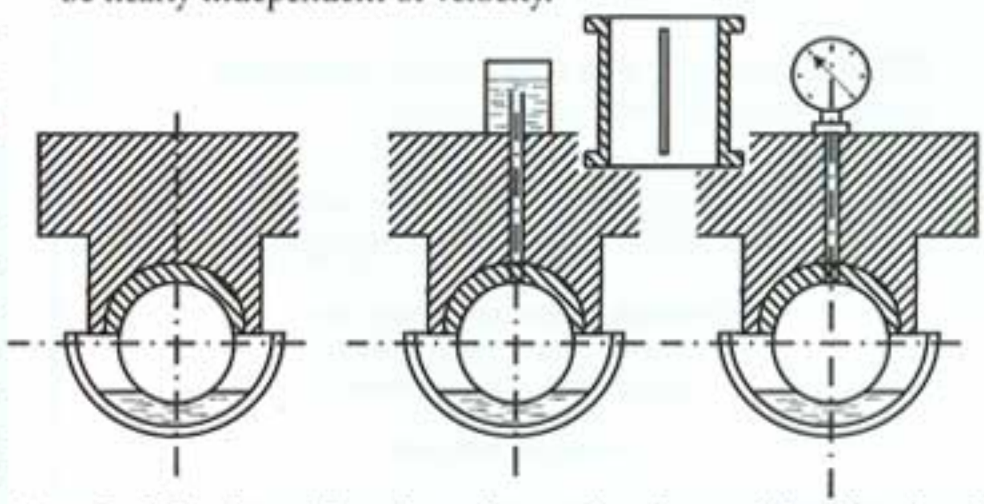

Figure 1. A drawing of Tower's early experiment examining the role of lubrication on railway axle bearings.

Tower experimented by immersing the shaft in a bath of oil. He found that the coefficient of friction between the axle and bearing varied greatly with rotational velocity. Tower drilled a feed hole into the top of the bearing cap and was surprised to see that oil traveled up the feed hole and could not be contained even after he tried to plug the hole with a wooden stopper. In effect, Tower discovered that the load of the shaft was carried need for durable and efficient bearings. In 1883, the Institution of Mechanical Engineers hired Englishman Beuchamp Tower to find the best way to lubricate railcar wheel bearings.

The illustration in Figure 1 shows the test rig Tower used to simulate the conditions found on railcar bearings. Previous researchers had erroneously believed that the load was carried by a pressure distribution in the oil film. Upon further study, he realized the summation of local hydrodynamic pressures multiplied by the projected area equaled the load supported by the bearing. Tower is generally credited with the discovery of hydrodynamic lubrication.

Further work by Sir Osborne Reynolds observed that hydrodynamic action was dependant on lubricant viscosity. Reynolds postulated that the lubricant adhered to the surfaces of the rotating shaft and stationary bearing and was dragged into the narrow clearance of the offset shaft forming a "pressure wedge" sufficient to carry the applied load.

Reynolds published the famous "Reynolds Equation," providing the mathematical model for oil pressure distribution in a hydrodynamic bearing. Hydrodynamic bearings are properly classified as "internally pressurized" because the pressure wedge is built up in the bearing clearance by the relative motion between the bearing and shaft.

During this same period, an exhibit was presented at the Paris Exhibition of 1878 called *Le Chemin de Fer de Glace* (Ice Railroad). This exhibit turned out to be one of the first examples of hydrostatic lubrication. The exhibit consisted of a large metal statue with four hollow legs on a flat steel plate. Oil was pumped down each leg with enough force to "float" the statue. The heavy statue could be moved with ease because the friction between the feet and the plate was greatly reduced by the thin oil film separating the two surfaces.

Hydrostatic lubrication applied to journal bearings can support load even with little or no relative motion between the rotating and stationary parts of the bearing because it uses external pressure to form the supporting layer of fluid. A modern example is high pressure "jacking oil" systems (usually Vickers pumps) used to reduce wear on start-up of large turbines. Hydrostatic journal bearings are fully lubricated around 360-deg of the bearing surface and tend to operate at relatively low eccentricity (near the center of the bearing clearance).

As technology advanced and rotating speeds increased in the early 20th century, many machines exhibited unstable behavior and high vibration. Experiments showed that flooding simple sleeve bearings with lubricant caused the bearings to exhibit instabilities. These fluid instabilities became known as *whirl and whip phenomena*. Whirl and whip instabilities are characterized by high sub-synchronous vibrations commonly occurring at a frequency just below 50 percent of running speed.

Since fluid instability was associated with flooded bearings, it was erroneously assumed that a fully lubricated hydrostatic bearing would be inherently unstable. To improve stability, bearings were operated partially lubricated at low pressure. High pressure, hydrostatic lubrication was avoided for all but the slowest speed applications. Over time, several features such as the axial groove, elliptical, offset half, pressure dam, and tilt pad were added to the plain hydrodynamic journal bearing in order to raise the instability threshold. These features helped but

is directly proportional to the force applied ($F = K \cdot d$). Dynamic rotating systems are a little more complex than simple static spring systems where the stiffness is represented by a single spring constant (K). On a rotating shaft where the rotor mass is supported by fluid bearings, the radial motion can be represented by the following equation:

$$r = \frac{\Sigma F}{\Sigma DS}$$

Where: r represents the radial displacement or vibration vector
ΣF represents the sum of the force vectors
ΣDS represents the dynamic stiffness vector

Because we are operating in a rotating system, we define the quantities in polar coordinates. Each term can be described by a vector with a magnitude, r, and phase angle, δ. If we trace the value of r over time, we obtain an orbit plot that represents the path that the shaft centerline takes through space. In practice, the orbit can be monitored using two orthogonally mounted proximity probes near the shaft surface. A Keyphasor® signal gives us a once per turn reference point that can be superimposed on the orbit to give us important information about the phase angle of the vibration vector.

The sum of the force vectors includes all of the forces acting on the rotor system. These forces can be static (unchanging in direction and time) or dynamic (exhibiting changes in magnitude or direction with time). Common examples of forces on rotor systems are gravity (static force) and unbalance (dynamic force).

The dynamic stiffness is derived from Newton's Second Law: The sum of forces acting on a body equals the mass times acceleration. By making certain assumptions – the rotor system parameters are isotropic, gyroscopic and fluidic inertial effects can be ignored, and linearity – we can create a simplified equation of motion based on the free body diagram (see Figure 2).

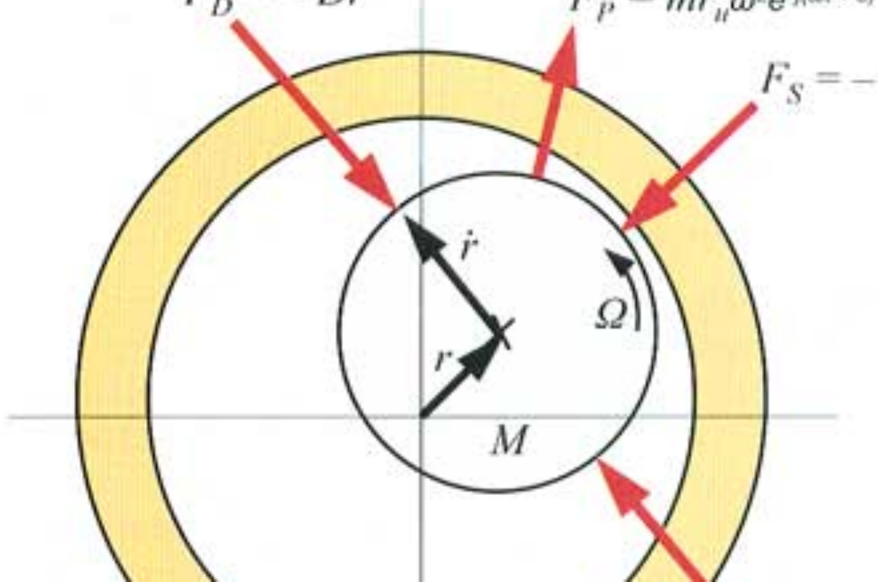

were never able to fully solve the problem of fluid instability.

The Rotor Model, Dynamic Stiffness, and Fluid Instability

Rotor systems can be modeled as spring systems using Hooke's law. Hooke's law states that the static displacement of a spring

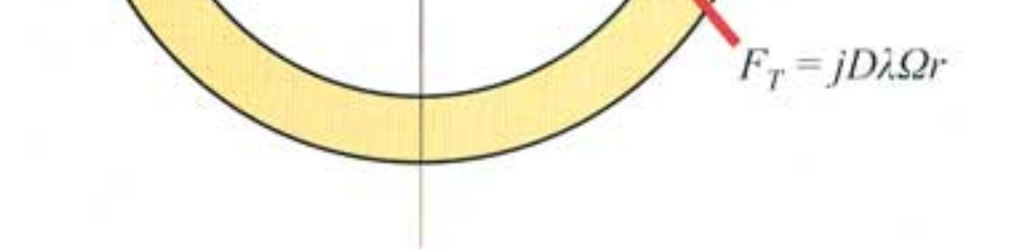

Figure 2. A free body diagram for a simple rotor system.

The free body diagram shows a rotor with mass M, rotating at a speed Ω, in a direction X to Y. The displacement from equilibrium is represented by the term r, velocity by the term $\dot{\mathbf{r}}$, and acceleration by the term $\ddot{\mathbf{r}}$. The spring term F_S points back toward the equilibrium position, the damping term F_D acts opposite to the velocity vector and the tangential stiffness force F_T in the same direction as the velocity vector. The perturbation force F_P is shown acting at angular position δ at frequency ω. The term mr_u represents the unbalance mass (m) operating at distance (r_u) from the center of the rotor. Newton's Second Law sets the sum of these forces equal to the mass M times the acceleration. Rearranging this equation to solve for dynamic stiffness results in the following:

$$\Sigma DS = K - M\omega^2 + jD\omega - jD\lambda\Omega$$

As shown in Figure 3, dynamic stiffness can be viewed as the sum of four vectors.

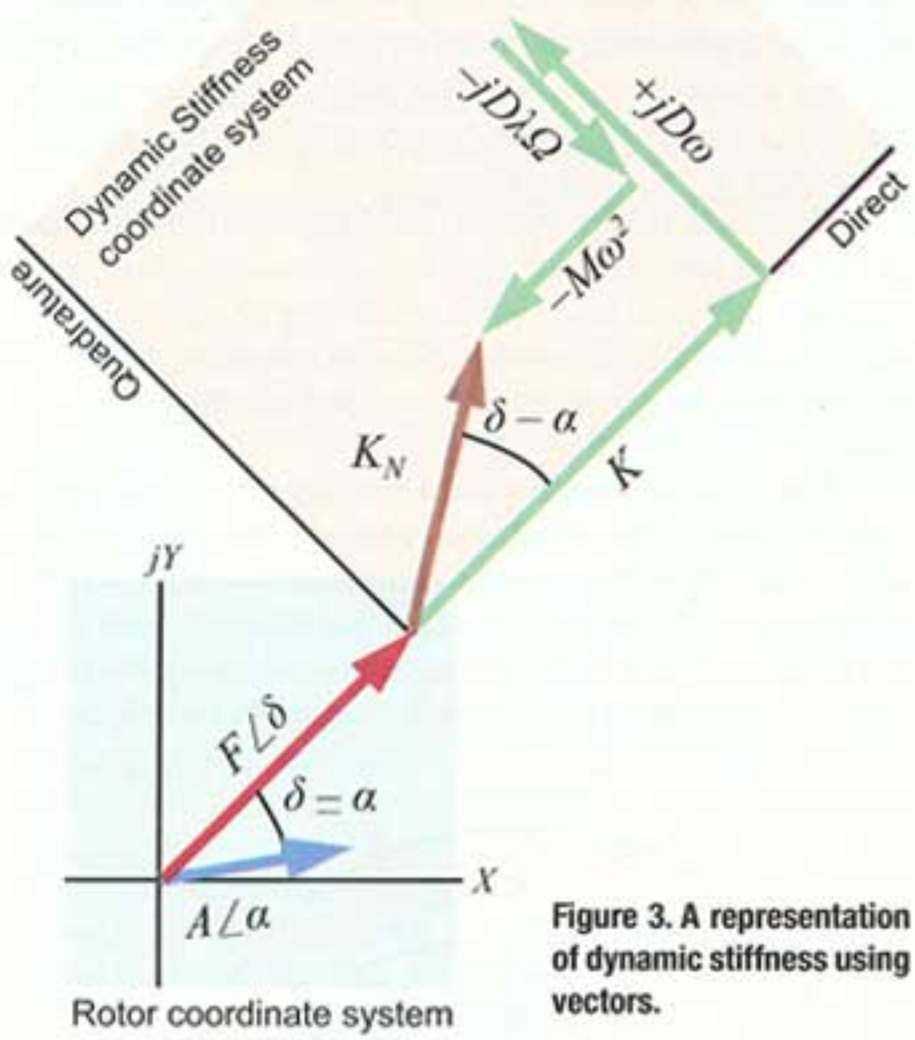

Figure 3. A representation of dynamic stiffness using vectors.

The four components of dynamic stiffness can be described in physical terms. The first term, K, is the simple spring constant. The positive value of K indicates that it acts opposite to the direction of applied force. The second term, - Mω2 is the mass stiffness that occurs because of the inertia of the rotor. The fact that this term is negative indicates it has a destabilizing effect on the rotor. The tangential stiffness term, - jDλΩ acts opposite to the damping term and is potentially destabilizing. The tangential stiffness term is proportional to the fluid circumferential angular velocity, λΩ.

The tangential stiffness term introduces the term lambda (λ) to our rotor model. Lambda describes the fluid circulation around the circumference of the bearing journal. Whenever a viscous fluid is contained between two surfaces moving at different velocities, the fluid will be dragged into relative motion. Because of friction, the relative velocity of the fluid at the surfaces will be zero. Because the surfaces are moving at different rates, the fluid will develop a velocity profile similar to the one represented in Figure 4.

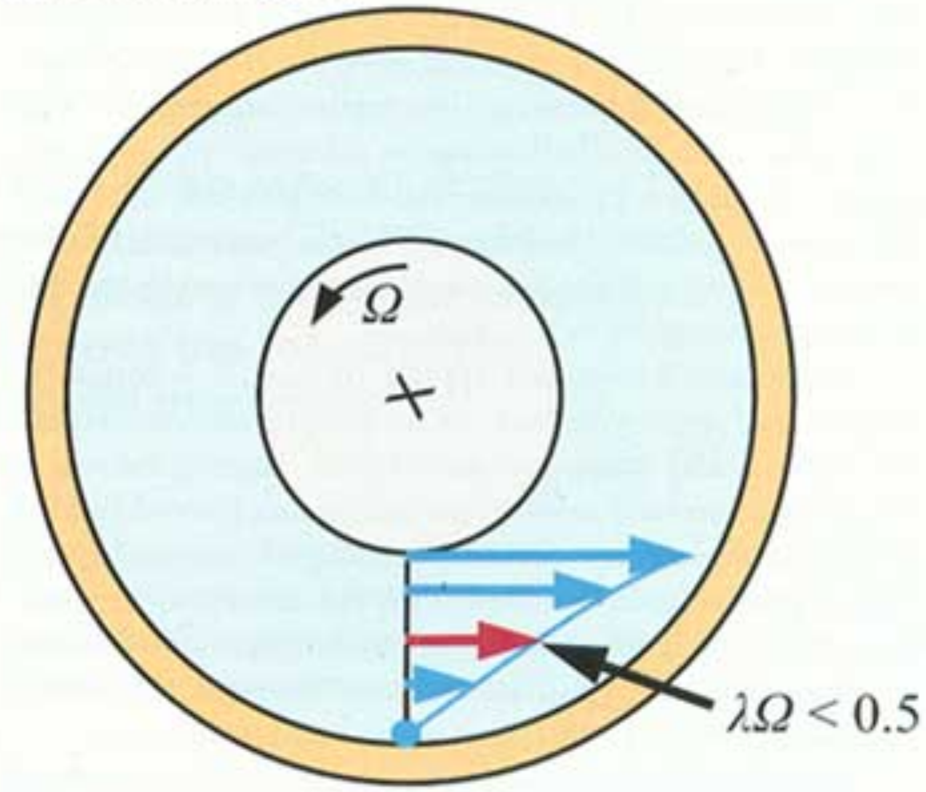

Figure 4. The average fluid angular velocity is represented by λΩ.

If we return to our equation for radial position of our spring-mass-damper system,

$$r = \frac{\Sigma F}{\Sigma DS}$$

the maximum displacement will occur when the value of dynamic stiffness is small for any non-zero value of applied force. Instability, defined as the threshold where r becomes bounded only by the mechanical constraints of the system and non-linear effects, occurs when the value of the dynamic stiffness in our model equals zero.

Because the dynamic stiffness consists of both direct and quadrature terms, this condition is satisfied when K = Mω2 and ω = λΩ. Combining these two conditions results in the Bentlying effect on the rotor system. Both of these terms are known as direct terms because they act in parallel to the direction of applied force. The third and fourth terms used in this equation are known as quadrature terms. These terms are preceded by the symbol j to indicate that they act at 90-deg to the direction of applied force. The term $jD\omega$ is the fluid damping term. The fluid damping term is positive, indicating that it has a stabiliz-

Muszynska formula for the Threshold of Instability:

$$\Omega_{TH} = \frac{1}{\lambda}\sqrt{\frac{K}{M}}$$

This simple equation provides an excellent starting point for comparing the stability of different fluid bearing designs.

The Bently-Muszynska model predicts that the stiffer the bearing support and the lower the value of lambda, the higher the Threshold of Instability or stability margin.

Root Locus Stability Analysis

The best way to evaluate the stability of rotor systems and bearing designs is to use a graphical technique known as the Root Locus Method. This method graphs the roots of the characteristic equation of the rotor system:

$$M\ddot{r} + D\dot{r} + (K - jD\lambda\Omega)r = 0$$

The solution of the characteristic equation takes the following exponential form:

$$r = Re^{st}$$

Solving for s in the case when R, λ, and Ω are non-zero we obtain two complex roots.

$$s_1 = \gamma_1 + j\omega_d \quad \text{and} \quad s_2 = \gamma_2 - j\omega_d$$

Because the solution for r (displacement) has an exponential form, values will grow unbounded with time when the roots are positive and decay when the roots are negative. Negative roots indicate that the rotor system is stable and will return to an equilibrium position when disturbed. Positive roots indicate instability. No real machine can operate in the region of instability. When the roots equal zero, r will remain constant. This represents behavior at the Threshold of Instability. Figure 5 shows a typical root locus plot over a range of operating speeds from 0- to 1000-rad/s. Based on this plot, the predicted threshold of instability is expected to be 870-rad/s.

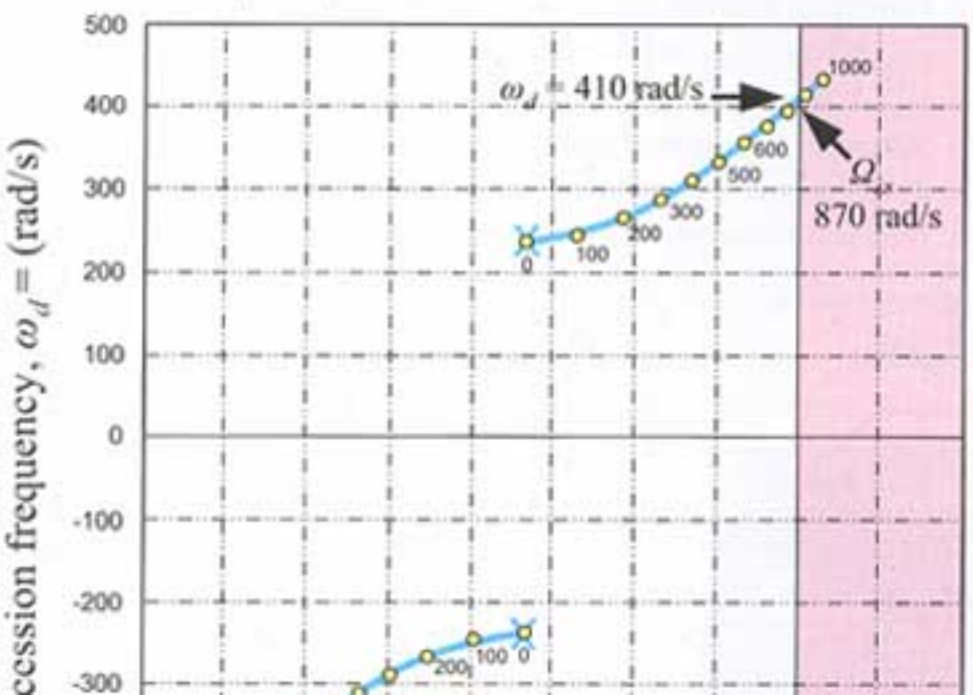

Root Locus plots can be used to evaluate the effect on stability for a wide range of machine parameters, making it an extremely useful tool for rotordynamic analysis.

The Externally Pressurized Bearing (EPB)

In contrast to hydrodynamic bearings that rely on the relative motion between the rotating journal and stationary bearing to create a pressure wedge to support the load of the shaft, externally pressurized bearings (EPB) rely on an externally generated source of pressure. Therefore, they have several unique features and advantages that make them superior to the low pressure hydrodynamic journal bearings and even the latest modified geometry bearings such as the lobed and tilt-pad bearings.

The distance to the bearing wall is measured by the eccentricity ratio (0 represents a centered journal, 1 a journal touching the bearing wall). As seen in Figure 6, a hydrodynamic sleeve bearing must operate off center to create the pressure wedge that supports the bearing load. The stiffness of the hydrodynamic bearing is affected by the eccentricity ratio, which is lowest when the eccentricity ratio is near zero. Misalignment during installation or changing radial loads can result in a hydrodynamic bearing that is forced to operate at low eccentricity ratio and low stiffness. Since we showed earlier that the threshold of instability and the vibration response is related to stiffness, a normally stable hydrodynamic bearing can have problems when operating at low eccentricity ratio.

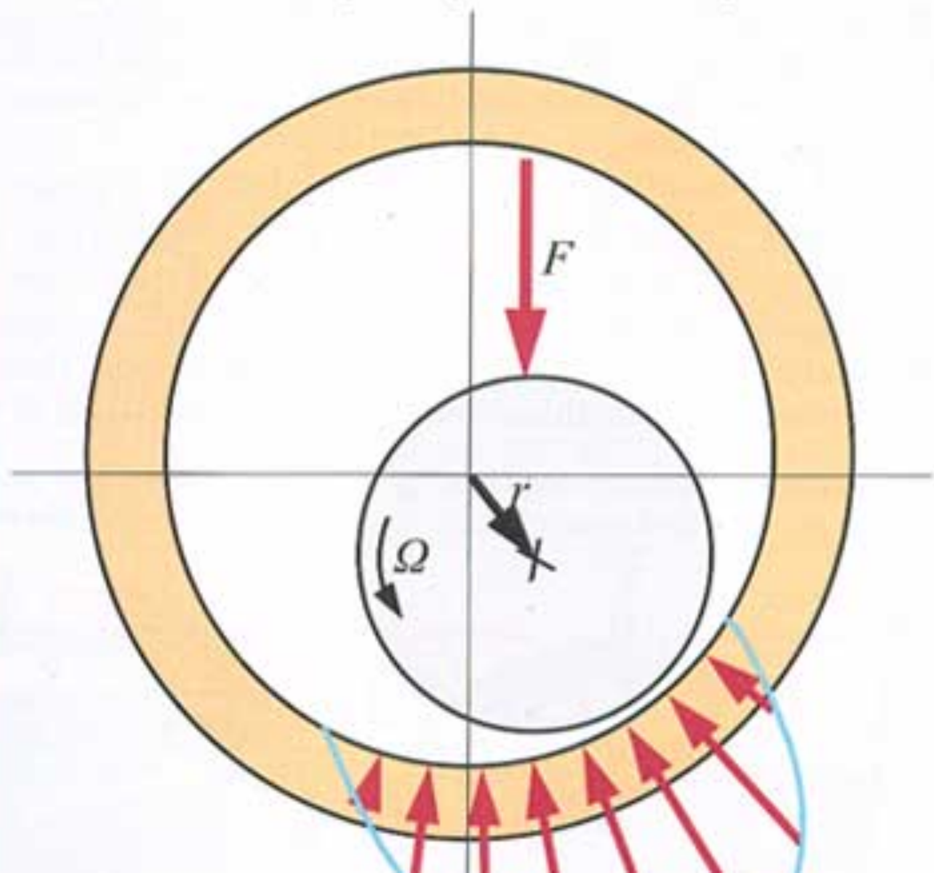

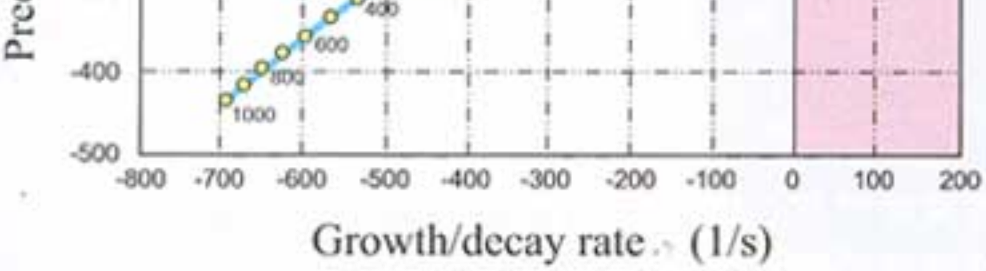

Figure 5. A Root Locus plot showing the forward and reverse precession roots.

Figure 6. A pressure wedge supports the load of a hydrodynamic bearing operating at high eccentricity.

Because its stiffness derives from external pressure, the EPB can retain good stiffness and damping properties even at low eccentricity ratio. The relationship between eccentricity ratio and bearing stiffness for several bearing types is shown

in Figure 7. While both the EPB and the hydrodynamic bearings have good relative stiffness at high eccentricity, only the EPB retains its stiffness at zero eccentricity. A pure hydrostatic bearing operating at very slow speed has good stiffness at zero eccentricity but does not have the advantage of hydrodynamic lubrication at high eccentricity.

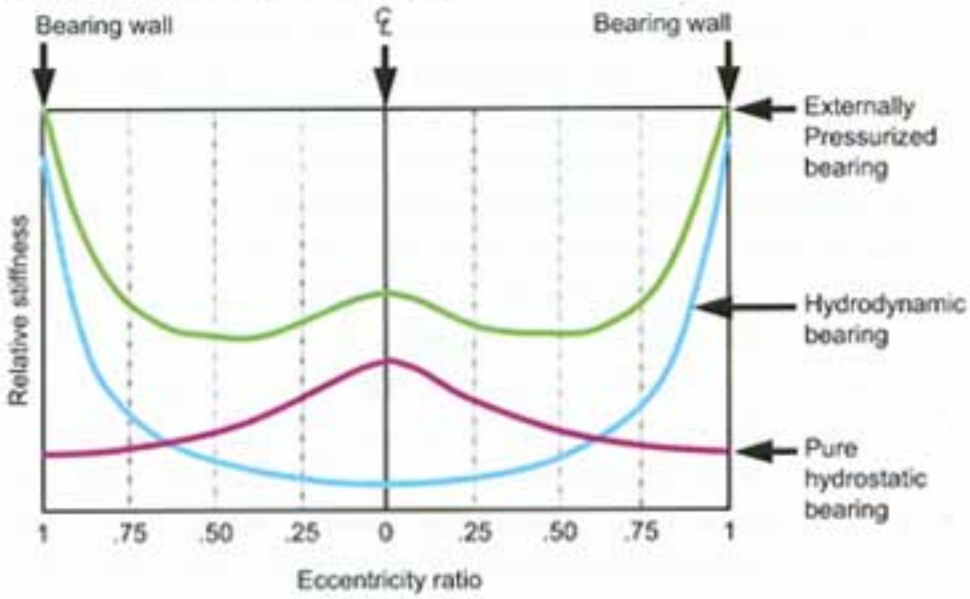

Figure 7. Relative stiffness as a function of eccentricity ratio.

The superior stiffness value of the EPB makes it less prone to instability even when subject to misalignment, changing radial loads, or operation at low eccentricity. This feature of the EPB makes it ideal for installation on vertical machines found in many large hydro installations. In vertical hydro turbines, the lack of gravity side load makes it possible for the guide bearing journals to be forced to operate at low eccentricity. This is often the case during transient loading conditions that occur during start-up or shut-down.

Figure 8 show the typical pressure profile of a four pocket EPB design. The pressure profile around the EPB differs from the low pressure bearing because it acts around 360-deg of the circumference. The unique feature of the EPB is the pressure profile that acts along the longitudinal axis of the bearing. This axial pressure gradient drives flow out the end boundaries of the bearing geometry, effectively reducing the value of lambda (average circumferential velocity ratio).

External pressurization controls stiffness and lambda, the two parameters that directly contribute to the stability of the bearing. Not only are these two parameters controllable during the bearing design process but they are also controllable by the operator "online." The properties of the bearing can be changed after installation by changing the external supply pressure (stiffness and lambda) or the supply temperature (damping).

Almost all types of hydrodynamic bearings in use today rely on petroleum based lubricating oils. Physical properties of lubricating oils facilitate the formation of the pressure wedge that supports the load in the internally pressurized bearing. Water has poorer lubricant properties and does not work well in hydrodynamic bearings. The EPB can operate with conventional petroleum lubricants but can also operate with other incompressible fluids such as water. Water can be used to support load in the EPB because the internal pressure profile is dependant on an external pressure source and not primarily the relative motion between bearing and journal. The EPB opens the possibility of choosing a bearing fluid not solely on its lubricant properties but also for its compatibility with the process and the environment.

In hydro power applications, two convenient sources of pressurized water can be used to supply the EPB. If a clean water source with sufficient head is available from the penstock, it may be used to supply the EPB. Typically, filtration in the 3 to 5 micrometer range is necessary to protect the close tolerances of the EPB. The pressure necessary for the operation of the EPB must be calculated by the bearing designer on a case by case basis. Typically, the pressure needed is in the range of 150-psi to 1000-psi, or between 350-ft and 2300-ft of static head.

If a suitable source of water is not available from the environment, pressurized water can be produced by a closed loop fluid delivery system. The fluid delivery system is composed of several components, typically a high pressure pump, a high pressure filtration unit, and a low pressure pump and heat exchanger on a kidney loop to control the fluid temperature. Sensors are employed to monitor the fluid temperature, pressure, and flow. Controls and interlocks can be employed to insure that the bearing is operating at the desired design conditions. A pressurized accumula-

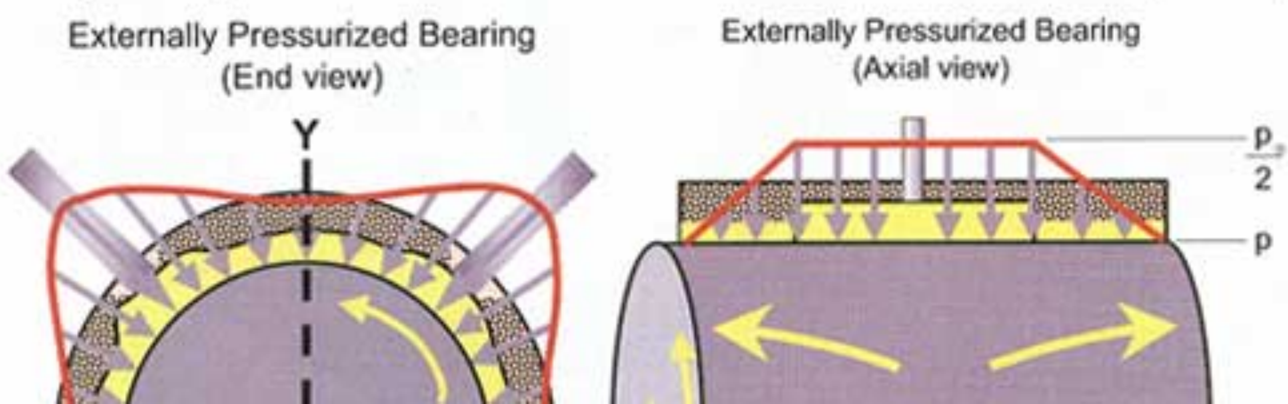

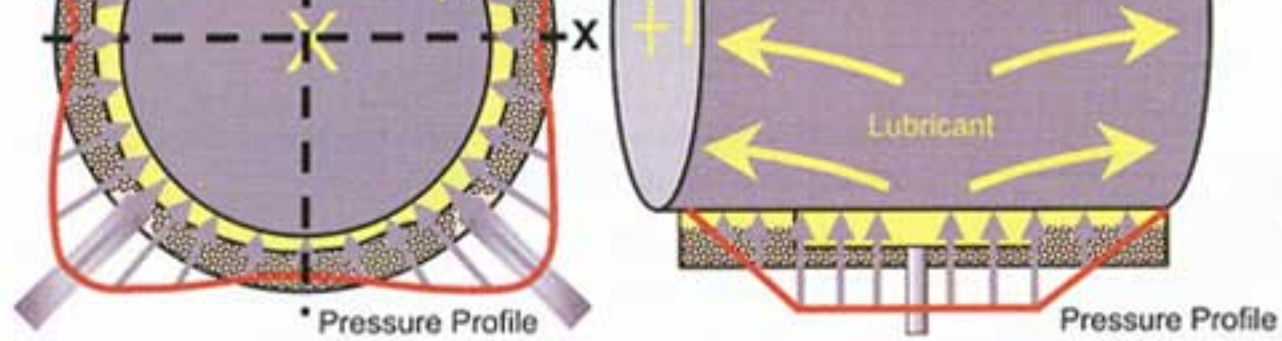

Figure 8. The pressure profile of a four pocket externally pressurized bearing around the circumference (end view) and along the longitudinal axis.

tor is generally employed to allow for a controlled shutdown of the machine should the system experience a sudden loss of pressure for any reason.

Field Data Collection

To obtain baseline data for the hydrodynamic oil bearings, field data was collected from a hydro turbine at Southern California Edison's Lytle

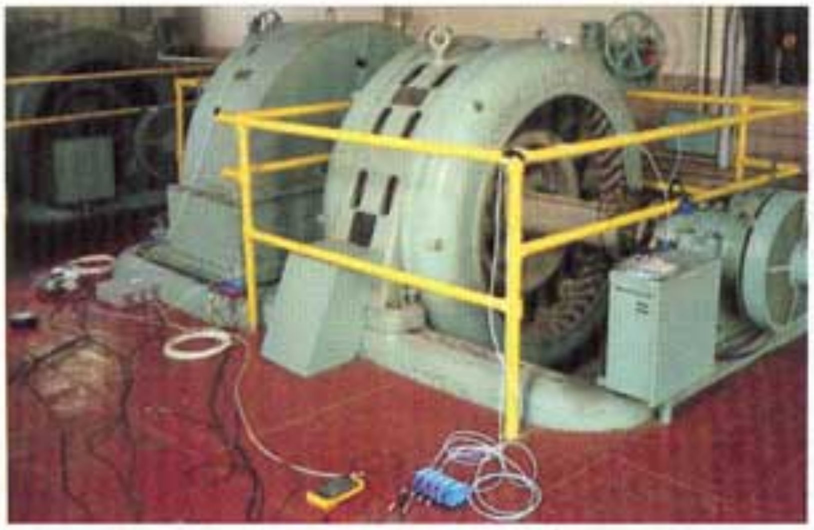

The Pelton wheel (left) and generator (right) instrumented with temporary proximity probes for diagnostic analysis.

The center pedestal (Bearing 2) in close proximity to the Pelton wheel (right).

Creek generating facility. A typical machine train is composed of two major components: a Pelton water wheel and a General Electric three-phase generator. The generator and Pelton wheel are mounted on a common horizontal shaft supported by three bearings. Bearing 1 is located outboard of the Pelton wheel, bearing 2 is located between the Pelton wheel and the generator, and bearing 3 is located outboard of the generator.

The bearings appear to be those supplied with the original equipment. They utilize soft metal babbitt faces with diagonal grooves to help distribute the oil. Soft metal is used to avoid damaging the shaft upon start up and shut-down. A leather slinger is employed on the shaft to contain the oil in the bearing pedestal. Based on nameplate information, it appears that the Pelton wheel and generator were manufactured in 1909.

A common occurrence on these types of machines is oil leakage from the bearing pedestals. This problem is prevalent at bearing 2 which is in close proximity to the Pelton wheel. The housing of the Pelton wheel operates under slight vacuum, causing oil to be sucked into the water discharge. Bearing 2 also carries most of the load of the machine. For these reasons, it was decided to replace the hydrodynamic oil bearing in the middle of the machine with an externally pressurized water bearing.

Because of the historical nature of these machines, Southern California Edison requested that no external modifications be made to the bearing pedestals. The EPB retrofit which consisted of new bearings and backers was designed to fit inside the original pedestal with small penetrations for pressurized water delivery and return.

Properties of Original Oil Bearing	
Length	18 inches
Diameter	6 inches
Bearing construction	Babbitt lined steel with diagonal oil grooves.

The field data collected from this machine revealed no surprises. The machine appeared to be well behaved and exhibited

Test Stand Data

To validate the pressurized water bearing design, a near full-scale model of the turbine generator machine train was constructed in Minden, NV. The original number 2 bearing pedestal from Southern California Edison's Mill Creek site was used to support a pressurized water bearing and replacement backer. The simulated machine train uses two rotating wheels with a weight of 3,300-lb each to model the turbine and generator. The total rotating weight with shaft is close to 8,000-lb. The shaft is driven by a variable speed electric motor at 450-rpm. Two roller bearings are used on either side of the wheels to simulate bearings 1 and 3.

The test stand pressurized water bearing was designed to carry slightly more than half the total load. Pressurized water is prises. The machine appeared to be well behaved and exhibited rotor dynamic data consistent with a heavy, slow speed horizontal machine. Proximity probes mounted near the bearing housings and a once per turn Keyphasor® signal were used to generate the orbit plot shown in Figure 9. Plot #223 shows the filtered 1X (synchronous) vibration, a nearly circular orbit with 2-mil peak to peak vibration. Field data from the number 2 bearing was difficult to interpret due to axial movement over a taper in the shaft at the probe locations. Field data from bearing 1 was reported as representative of the shaft vibration.

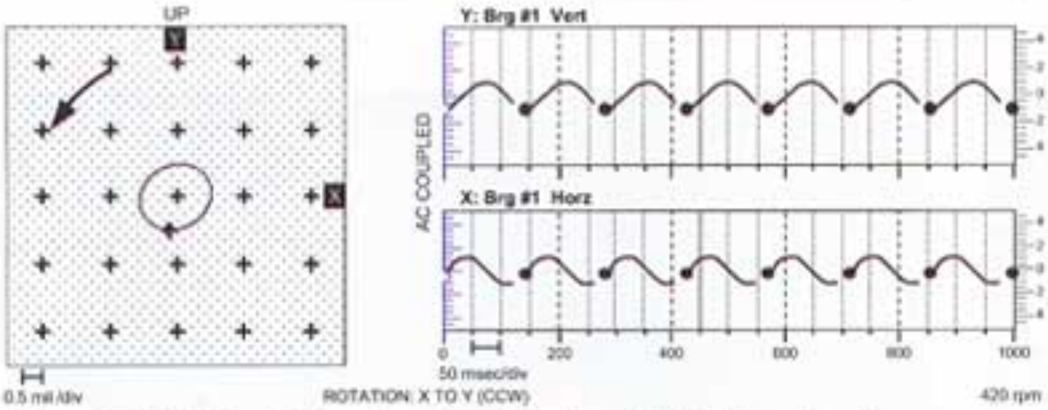

Figure 9. 1X Orbit plot from bearing 1 (outboard of Pelton wheel).

The data plot shown in Figure 10 is a transient data plot showing the average shaft centerline position from start-up to operating speed. This reveals a moderate rise in the shaft centerline, from minus 1.5-mil to +0.5-mil, over the speed range consistent with hydrodynamic bearing performance.

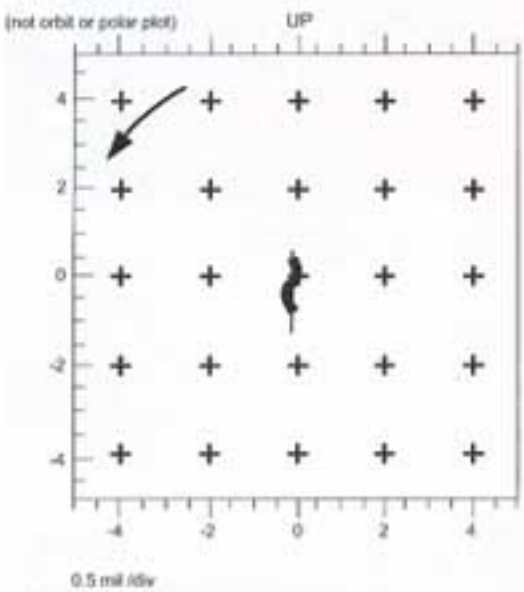

Figure 10. Average shaft centerline position of the original oil bearing.

generated by a closed loop fluid delivery system that supplies 15-gpm flow at 700-psi. The properties of the pressurized water bearing are as follows:

Properties of Pressurized Water Bearing	
Length	14 inches
Diameter	6 inches
Bearing construction	Bronze

Data collected from the test stand is shown below in Figures 11 and 12. The 1X filtered orbit shows a very small peak to peak vibration of about 1-mil. About 4-lb of unbalance mass was added to the drive end wheel diameter to obtain this vibration amplitude. Vibration without the unbalance mass (not shown) was almost undetectable. This data was used to calculate the stiffness value for the pressurized water bearing. The stiffness was estimated at 900,000-lb$_f$/in, significantly higher than the value of the original hydrodynamic oil bearing.

Similarly, the shaft centerline plots show very little change in position of the shaft centerline (shaft eccentricity) from start-up through running speed. Analysis of the full spectrum vibration plots (not shown) verifies that no abnormal sub-synchronous vibrations are present in the operating data. The data collected confirms that the EPB can operate near zero eccentricity with excellent stiffness and no sign of fluid instability.

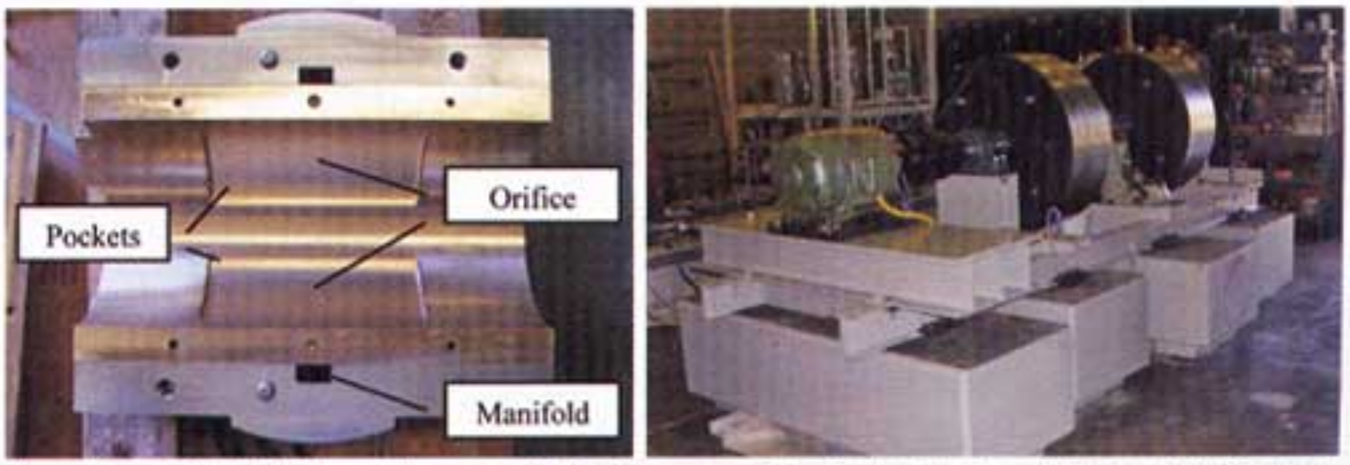

The photo on the left shows the upper half of the pressurized water bearing (the lower half is similar). Notice the hydrostatic pockets, orifice locations, and pressurized water manifold. The photo on the right shows the bearing test stand in Minden, NV.

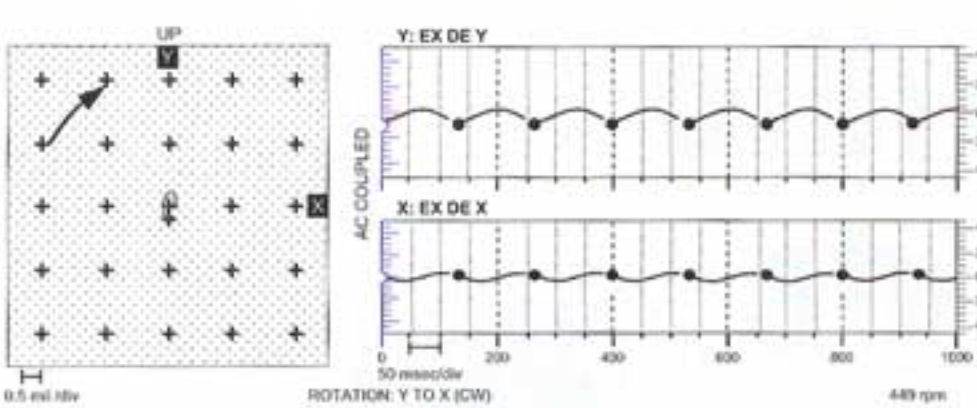

Figure 11. Shaft orbit at the DE (drive end) side of Bearing 2 pedestal.

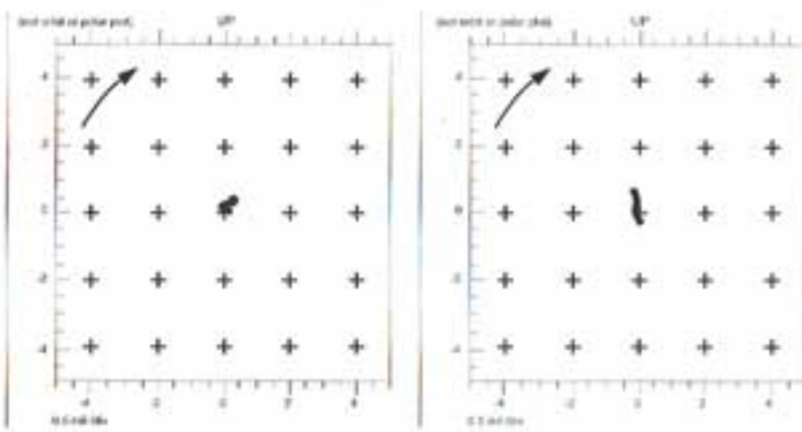

Figure 12. Shaft average centerline plot of test stand bearing 2.

Conclusions

The externally pressurized bearing solves the age old problem

in the many vertical configuration Francis turbines worldwide. Many potential applications of pressurized bearing technolof fluid bearing instability. It takes the century-old principles of hydrostatic bearing lubrication, and applies them in such a way that enhances bearing stiffness and reduces lambda. In doing so, the externally pressurized bearing can positively influence the two bearing factors that have the greatest impact on the stability of rotating machinery.

While this report details the application of the externally pressurized water bearing in a radial load application, the technology works equally well on vertical machines and can be successfully applied to thrust bearings, resulting in similar benefits and advantages. This makes application of the technology ideal ogy can be found in the power, petrochemical and industrial machinery markets. The simple principles described in this paper can be applied universally to high speed gas turbines using compressed gas bearings or low speed hydro turbines utilizing pressurized water or more traditional oil lubricated bearing systems.

P&S

Carlo F. Luri is the general manager of Bently Biofuels Company, 1711 Orbit Way, Minden, NV 89423, 775-783-0123, Fax: 775-783-4650, www.bentlybiofuels.com.

Pumps & Systems, December 2006

Back to Publications